Supplementary Information

Phosphine-based porous aromatic frameworks for gold nanoparticle immobilization with superior catalytic efficiency

Yuting Yang, Tienan Wang, Xiaofei Jing* and Guangshan Zhu*

Key Laboratory of Polyoxometalate Science of Ministry of Education, Northeast

Normal University, Changchun 130024, P. R. China.

*E-mail: zhugs@nenu.edu.cn

Instrumental characterization

Fourier transform infrared spectroscopy (FTIR) spectra (film) were measured using a Nicolet Magna 560IR spectrometer. Solid-state ^{13}C and ^{31}P cross polarization magic angle spinning nuclear magnetic resonance (CP/MAS NMR) measurements were performed on a Bruker Avance III model 400 MHz NMR spectrometer at a MAS rate of 5 kHz. X-ray photoelectron spectroscopy (XPS) was performed using a Thermo ESCALAB 250. Scanning electron microscopy (SEM) imaging was performed on a JEOS JSM 6700. Transmission electron microscopy (TEM) was recorded using a JEOL JEM 3010 with an acceleration voltage of 300 kV. Thermogravimetric analysis (TGA) was performed using a Perkin-Elmer TGA analyzer system at a heating rate of 10 ^{o}C min^{-1} in air. Powder X-ray diffraction (PXRD) was performed with a Siemens D5005 diffractometer with scanning rate of 4 ^{o}C min^{-1} (2θ). The gas adsorption–desorption isotherms were measured on a Quantachrome Autosorb-iQ2 analyzer. The conversion progress of 4-NP reduction was monitored by Cary 50 Conc UV-visible spectrophotometer.
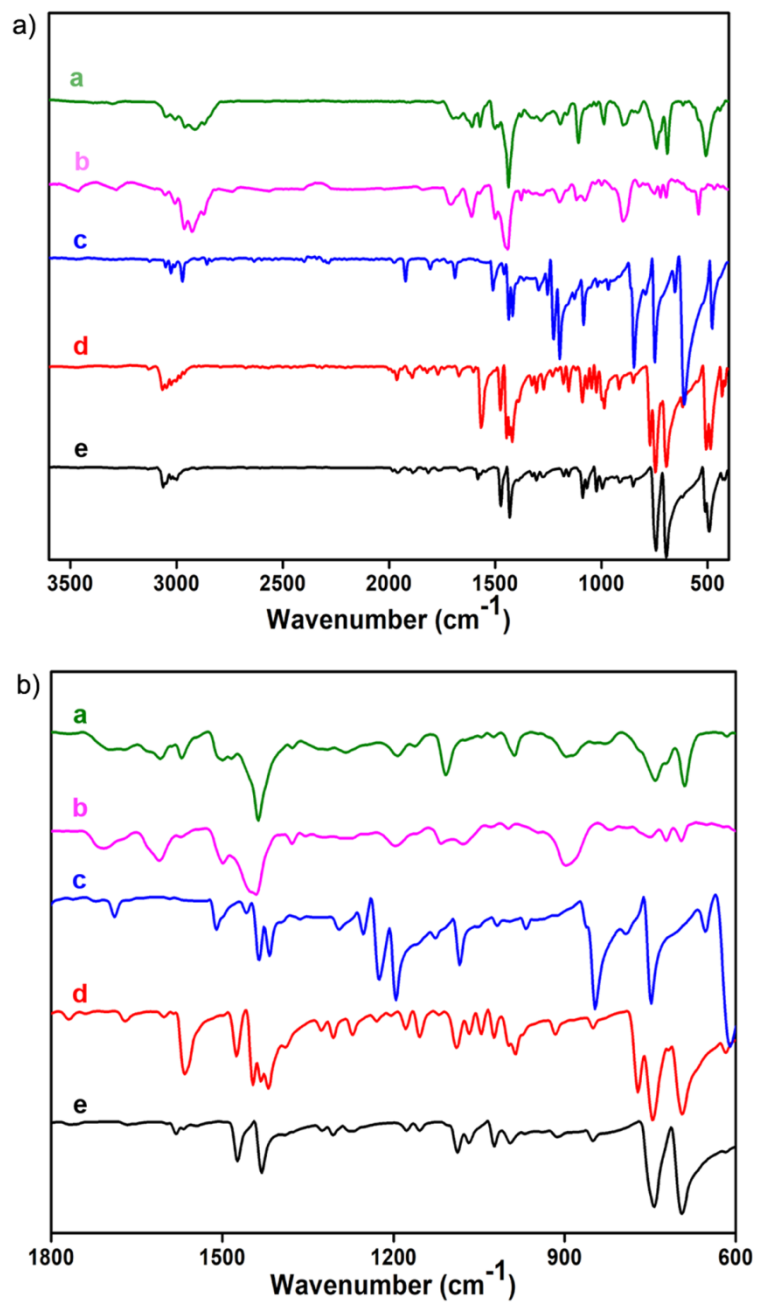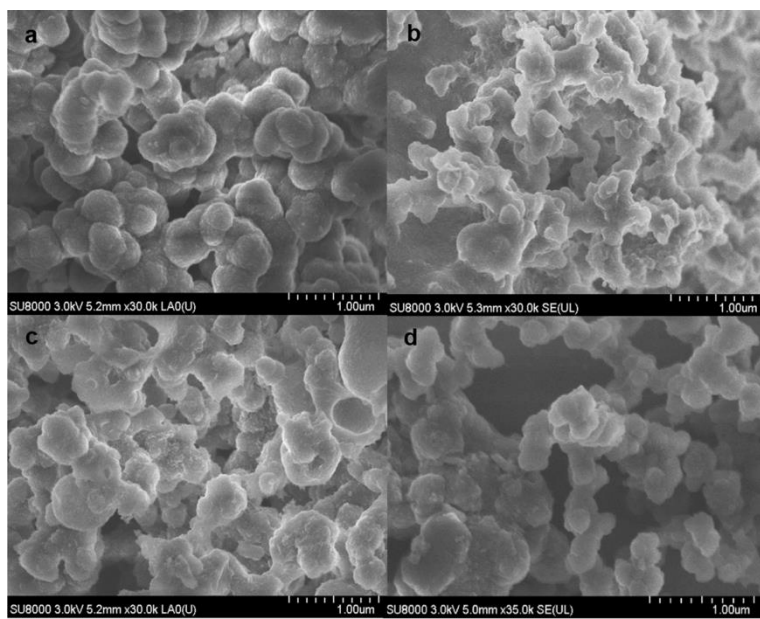
Fig. S1 FTIR spectra in the range of a) 4000-400 cm^{-1} and b) 1800-600 cm^{-1} of PPh$_3$ (a), PPh$_2$Py (b), DBpX (c), PAF-93 (e), and PAF-94 (f), respectively.
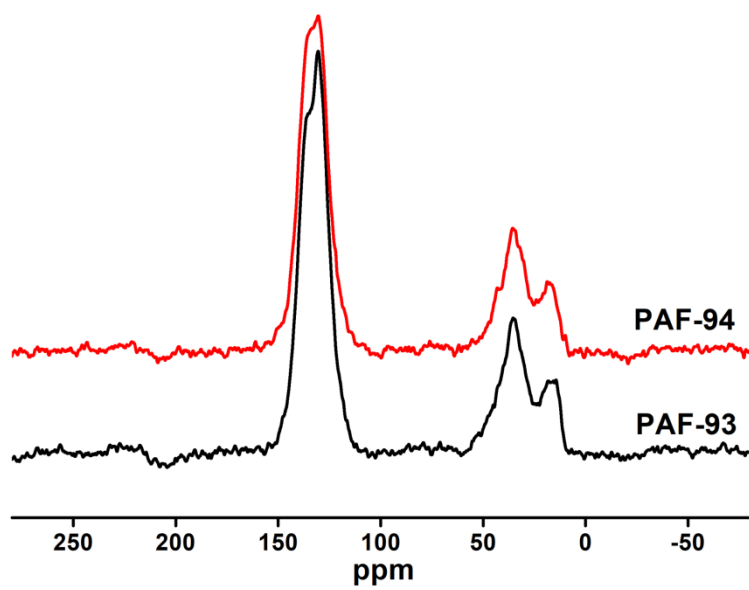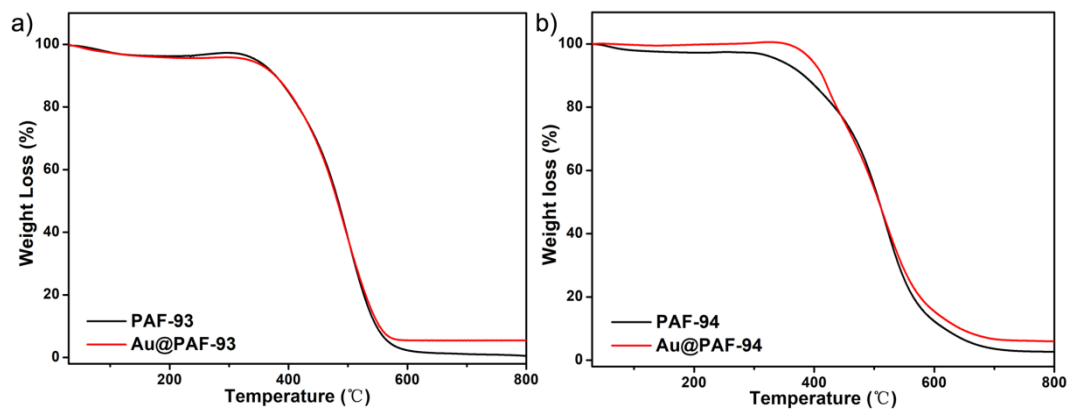
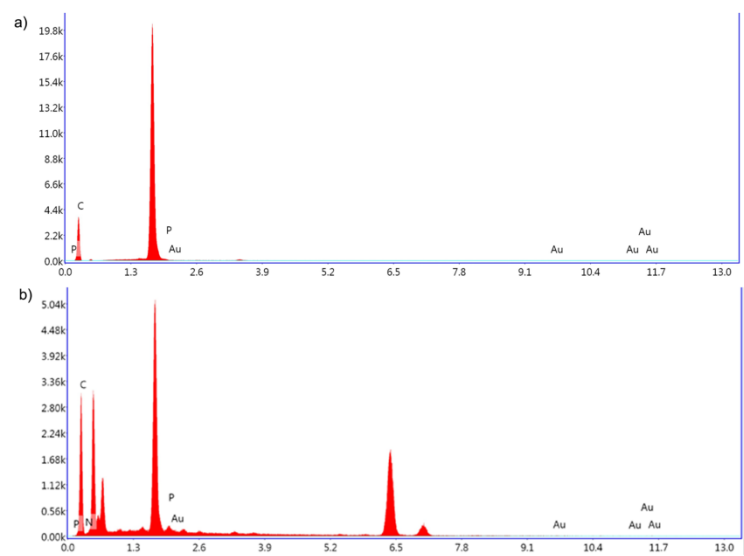**Fig. S2** ^{13}C solid-state NMR spectra of PAF-93 and PAF-94.
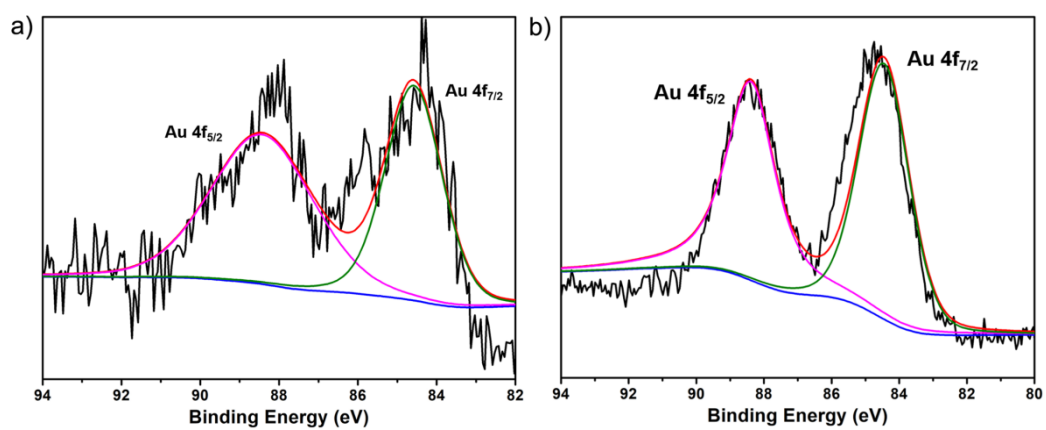
Fig. S3 Au 4f region in the XPS spectra of Au@PAF-93 (a) and Au@PAF-94 (b).
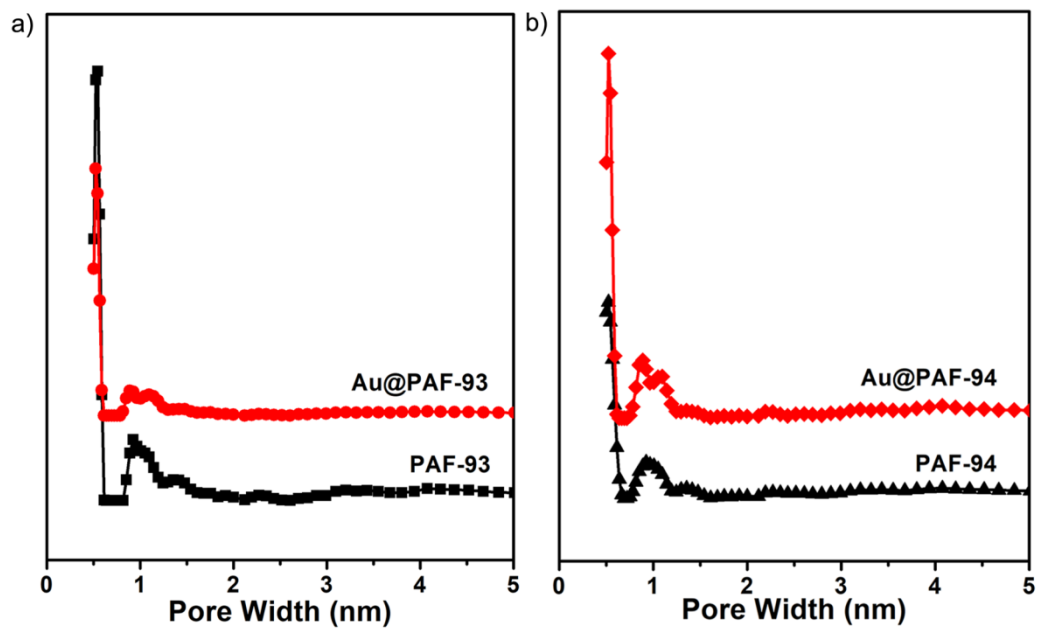
Fig. S4. SEM images of PAF-93 (a), Au@PAF-93 (b), PAF-94 (c) and Au@PAF-94 (d), respectively.

Fig. S5 TGA curves of PAF-93 (a), PAF-94 (b) and their corresponding Au@PAFs.
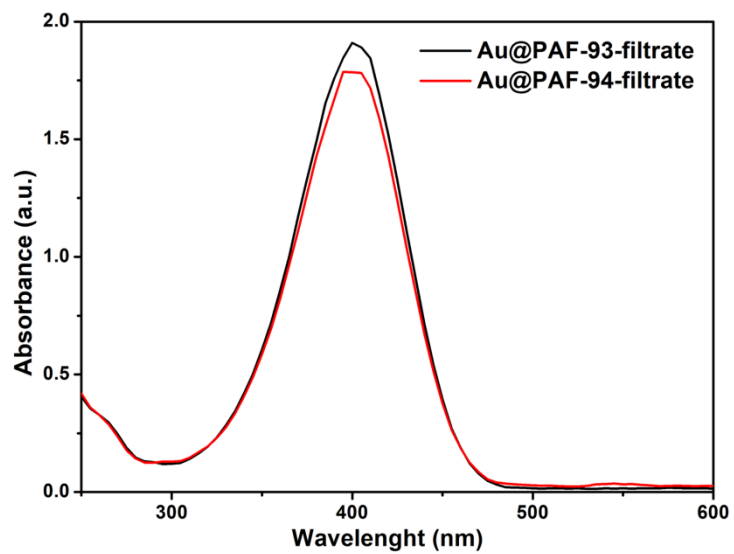
**Fig. S6** EDX spectra of Au@PAF-93 (a) and Au@PAF-94 (b).

Fig. S7 Pore size distributions of PAF-93 (a), PAF-94 (b) and their corresponding Au@PAFs.

Table S1 Summary of rate constants of other similar 4-NP reduction reactions catalysed by previously reported AuNPs catalysts with solid supports.

| Catalysts	Size (nm)	Au content (%)	Rate constant, k (s^{-1})	Reference
Au@TpPa-1	5	1.2	5.35×10^{-3}	26
Au@CPF-1	5	1.24	5.05×10^{-3}	35
Au/COF	13	0.2	7.66×10^{-3}	27
Au@CPOP	4.5±1.5	10.5	4.04×10^{-3}	47
Au@MIL-100	60	35.55	5.5×10^{-3}	48
Au@SiO$_2$	104±9	--	14×10^{-3}	13
Au/MgO	5-7	1.34	7.6×10^{-3}	49
Au@Ag/MOF	2-6	2	5.05×10^{-3}	17
Au@PAF-93	2.8±0.3	2.72	2.68×10^{-3}	This work
Au@PAF-94	1.9±0.4	4.25	22×10^{-3}	This work

Fig. S8 UV-vis spectra of the reduction of 4-NP after 30 min catalysed by the filtrate solution of Au@PAF-93 and Au@PAF-94 catalysts.
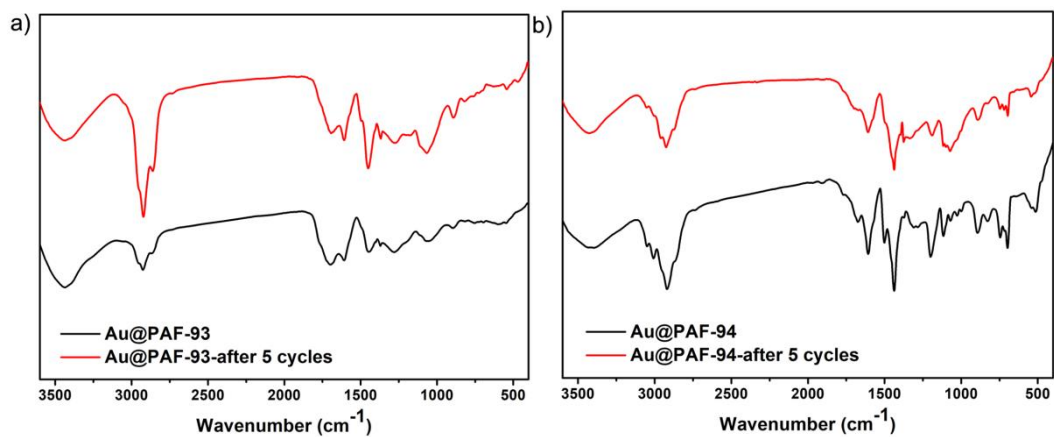
Fig. S9 FTIR spectra of fresh Au@PAF-93 (a), Au@PAF-94 (b), and their corresponding recycled Au@PAFs catalysts, respectively.
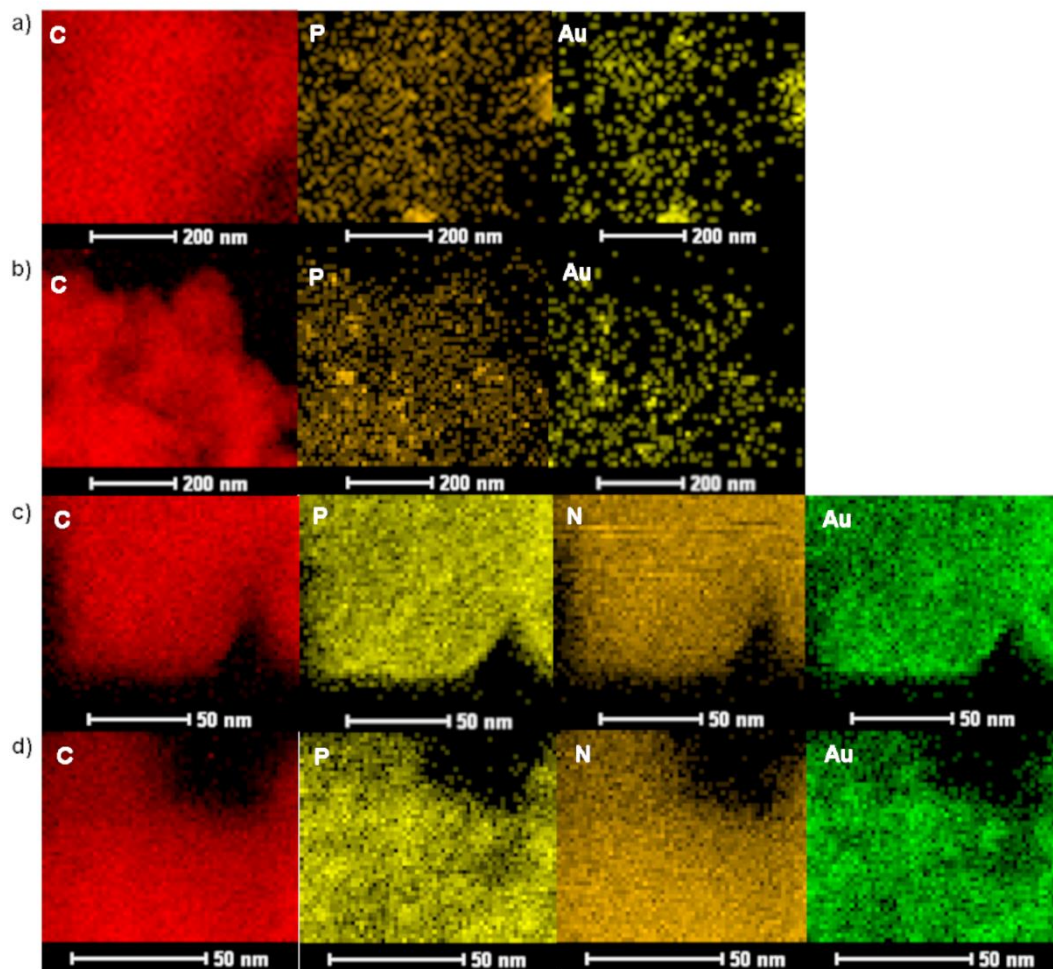
Fig. S10 TEM-EDX mapping images of fresh Au@PAF-93 (a), Au@PAF-94 (c), and their corresponding recycled Au@PAFs catalysts (b). recycled Au@PAF-93, d). recycled Au@PAF- 94), respectively.
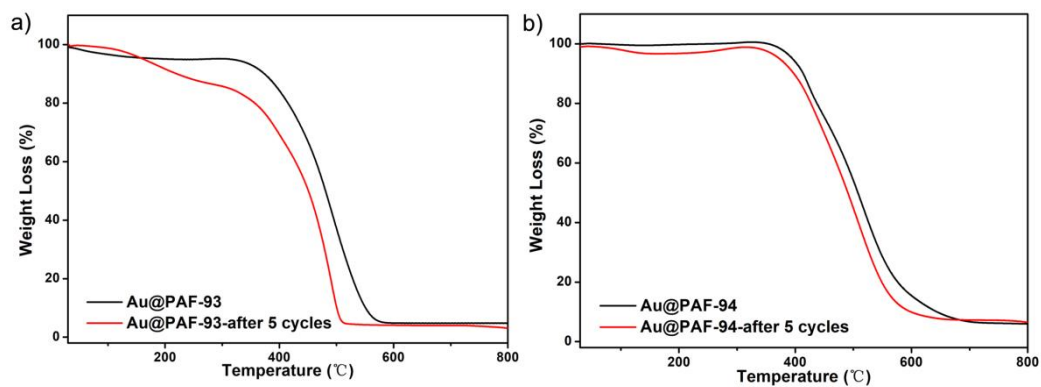
Fig. S11 TGA curves of fresh Au@PAF-93 (a), Au@PAF-94 (b), and their corresponding recycled Au@PAFs catalysts, respectively.